International Journal of Pure and Applied Mathematics
Volume 42 No. 3 2008, 391-397

VELOCITY FIELD CONSTRUCTION VIA LINEAR FINITE ELEMENT SOLUTION OF THE "DUAL FORMULATION" MODEL

Jun Cao[1 §], Peter K. Kitanidis[2]

[1]Department of Mechanical and Industrial Engineering
Ryerson University
Toronto, Ontario, M5B 2K3, CANADA
e-mail: jcao@ryerson.ca

[2]Department of Civil and Environmental Engineering
Stanford University
Stanford, CA 94305-4020, USA
e-mail: peterk@stanford.edu

Abstract: An accurate computation of flow in a heterogeneous isotropic formation is required in describing the advective transport of a contaminant. We present a novel method for velocity field construction using simultaneously linear hydraulic head and streamfunction solutions of the "dual formulation" flow model. A conservative advection-dispersion problem in a heterogeneous formation is solved for assessment of the accuracy of our new approach.

AMS Subject Classification: 76M12, 76S05
Key Words: finite element, "dual formulation" flow model, hydraulic head, streamfunction, advection-dispersion

1. Introduction

When using finite element methods to solve hydrogeologic problems associated with single-phase fully saturated flow in highly heterogeneous formations, an accurate finite element description of such groundwater flow is a prerequisite for achieving a reliable finite element solution to the subsequent solute transport problem. We adopt the "dual formulation" groundwater flow model (see [3]) to compute separately the hydraulic head, ϕ, and the steamfunction, ψ,

Received: August 17, 2007
§Correspondence author

via the simplest linear finite element descritization. Then, focusing on each individual triangular element, we can obtain the tangential velocity component at each of the three edges through application of the hydraulic head solution to Darcy's law; meanwhile, by using the streamfunction solution, we can also get the normal velocity component at the edge. Thus, at the common edge of two neighboring triangles, the tangential velocity component for one triangle could be different from that for the neighboring triangle (using Darcy's law to calculate velocity involves the conductivity which is, in our work, an elementwise distribution) while the normal velocity components for the neighboring triangles at their common edge keep identical (the conductivity is not needed in the computation of the normal velocity component using the streamfunction values). This ensures the conformity of flux across each element edge. The resulting tangential and normal velocity components within each triangular element are then transformed to an equivalent nodal-basis velocity expression, which eventually is used as the advective velocity in the transport problem. The advantage of our new approach in ensuring the conservation of the solute mass during its transport is demonstrated through comparison between two solutions to a conservative advection-dispersion problem using respectively the conventional method that relies on the hydraulic head solution only, and our new strategy that involves both hydraulic head and streamfunction solutions.

2. Modeling Equations

We use the linear triangular finite element method to solve two-dimensional flow and advective-dispersive transport problems within a rectangular domain Ω bounded by $L_{top} \cup H_{left} \cup L_{bottom} \cup H_{right}$. The first step is to compute the advective velocity using the *"dual formulation" flow* model, see [3]. The solution is obtained by separately computing the *hydraulic head* or *equipotential* (line of constant hydraulic head), ϕ,

$$\vec{\nabla}(K\vec{\nabla}\phi) = 0 \qquad \text{in} \quad \Omega \tag{1}$$

and the *streamfunction*, ψ,

$$\vec{\nabla}(\frac{1}{K}\vec{\nabla}\psi) = 0 \qquad \text{in} \quad \Omega\,, \tag{2}$$

where K, *hydraulic conductivity*, is taken as constant within each element in the numerical solution. The boundary conditions corresponding to (1) are:

$$\phi = \phi_1 \quad \text{on} \quad H_{left}; \quad \phi = \phi_1 \quad \text{on} \quad H_{right} \tag{3}$$

$$\frac{\partial \phi}{\partial n} = 0 \qquad \text{on} \quad L_{top} \cup L_{bottom}\,, \tag{4}$$

where $\vec{n}$ is an outwards normal unit vector at the boundary. Then, the Darcy flux (discharge per unit area of porous medium) is defined by:

$$\vec{q} = (q_x, q_y)^t = \left(-\frac{K}{\theta}\frac{\partial \phi}{\partial x}, -\frac{K}{\theta}\frac{\partial \phi}{\partial y}\right)^t \tag{5}$$

with θ denoting the porosity of the medium. We calculate the flux across either H_{left} or H_{right} via:

$$\Delta\psi = \int_{bottom}^{top} q_x(y)dy \tag{6}$$

and the boundary conditions for equation (2) can be set by:

$$\psi = 0 \qquad \text{on} \quad L_{bottom} \qquad \psi = \Delta\psi \qquad \text{on} \quad L_{top} \tag{7}$$

$$\frac{\partial \psi}{\partial n} = 0 \qquad H_{left} \cup H_{right}\,. \tag{8}$$

The second stage is to find the *concentration*, c, over time by solving the time-dependent advective-dispersive transport equation:

$$\frac{\partial c}{\partial t} + D_x\frac{\partial^2 c}{\partial x^2} + D_y\frac{\partial^2 c}{\partial y^2} + (\vec{u}\cdot\vec{\nabla})c = 0 \qquad \text{in} \quad \Omega\,, \tag{9}$$

where D_x and D_y are the principal components of the dispersion tensor; $\vec{u}$ is the groundwater flow velocity background obtained in the previous stage. The initial and boundary conditions of the concentration are:

$$c(x,y,0) = \begin{cases} c_o, & \text{within a certain small triangular element in } \Omega; \\ 0, & \text{elsewhere.} \end{cases} \tag{10}$$

$$\frac{\partial c}{\partial n} = 0 \qquad \text{on} \qquad L_{top} \cup H_{left} \cup L_{bottom} \cup H_{right} \tag{11}$$

respectively. More details about our finite element solvers used in this work can be found in [1] and [2].

3. Flow Field Construction

We solve equations (1) and (2) using the simplest piecewise linear interpolation. For each triangle τ, the effective conductivity is obtained by taking the geometric mean conductivity over τ. Thus, on the triangulation T, the elementwisely distributed conductivity is jumping between neighboring triangles. However, the piecewise linear finite element solutions of both ϕ and ψ remain continuous; also, streamlines and equipotential lines are perpendicular to each other owing

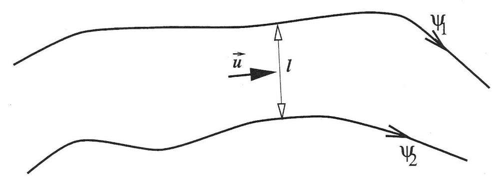

Figure 1: $\vec{u}$ in a streamtube

to the "dual formulation" flow model [3].

Through application of the hydraulic head solution to Darcy's law, we have:

$$\vec{u} = -\frac{K}{\theta}\vec{\nabla}\phi \tag{12}$$

Since we use the linear finite element approximation in the solution of the hydraulic head equation (1), applying equation (12) to a triangle yields only one constant velocity vector over the entire triangle. This will cause velocity jump between neighboring triangles. Consequently, the jump in the velocity calculated using (12) will be very likely to induce a local discontinuity for the velocity component that is pointing normal to the edge shared by two neighboring triangles, rendering the computed flux no longer conforming across their common edge. Thus, only using the linear hydraulic head solution is evidently inadequate for constructing a velocity background that can numerically secure flux conformity. On the other hand, while a streamtube formed by two streamlines $\psi = \psi_1$ and $\psi = \psi_2$ (see Figure 1) is locally examined at the segment l that connects the two streamlines and is also perpendicular to both streamlines (in other words, the segment l is located coincidentally on an equipotential line), the velocity is normal to the segment l with a magnitude:

$$|\vec{u}| = \frac{1}{\theta}\left|\frac{\psi_2 - \psi_1}{l}\right|, \tag{13}$$

where the computation does not involve the conductivity at all.

Based on the aforementioned observations, we propose a novel approach that makes use of both hydraulic head and streamfunction solutions to construct a physically flux-conformity-ensured flow field (see Figure 2). Here, we employ equation (13) for calculating the normal velocity component:

$$u_n = -\frac{1}{\theta}\frac{\psi_2 - \psi_1}{l} \tag{14}$$

while equation (12) is used to get the tangential velocity component:

$$u_\tau = -\frac{K}{\theta}\frac{\phi_2 - \phi_1}{l}\,. \tag{15}$$

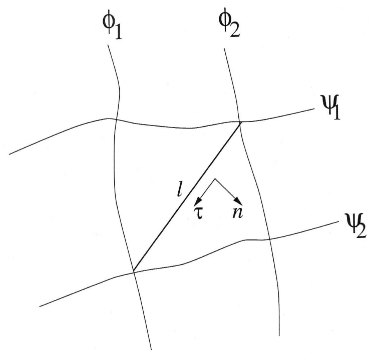

Figure 2: $\vec{u}$ in a flownet formed by streamlines and equipotential lines

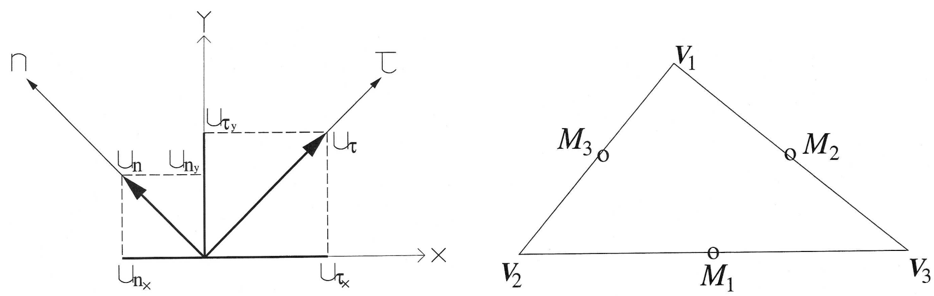

Figure 3: Transformations: from $\vec{u} = (u_\tau, u_n)^t$ to $\vec{u} = (u_x, u_y)^t$ (left) and from midpoints to vertices (right)

Note that if the edge l is the common edge of a pair of neighboring triangles, for the two triangles involved, the conductivity K could be different from each other since the effective conductivity on the triangulation is an elementwise distribution. This will result in the discontinuity of u_τ along the edge l according to (15). However, the normal velocity component u_n computed using (14) is independent of the conductivity K, which can guarantee the conformity of flux across the common edge of the two neighboring triangles.

With the velocity expressed in $\vec{u} = (u_r, u_n)^t$ at an edge, it is easy to transform it to $\vec{u} = (u_x, u_y)^t$ as in the standard Cartesian coordinate system (see left part of Figure 3). That is:

$$u_x = u_{\tau_x} + u_{n_x}, \quad u_y = u_{\tau_y} + u_{n_y}\,. \tag{16}$$

Then, the velocities at three midpoints of the three edges of the triangle τ, $\vec{u}_{M_1}$, $\vec{u}_{M_2}$ and $\vec{u}_{M_3}$, become available (see the right part of Figure 3). The following transformation:

$$\vec{u}_{V_1} + \vec{u}_{V_2} = 2\vec{u}_{M_3}, \quad \vec{u}_{V_2} + \vec{u}_{V_3} = 2\vec{u}_{M_1}, \quad \vec{u}_{V_3} + \vec{u}_{V_1} = 2\vec{u}_{M_2} \tag{17}$$

yields the $\vec{u}$ values at V_1, V_2 and V_3, three vertices of the triangle under examination. Thus, the standard linear finite element basis functions for $\vec{u}$ within triangle τ is ultimately formed, and will be used in the subsequent solute-transport computation.

4. Numerical Experiments and Discussion

We perform a numerical simulation of grundwater flow in a $0.4m \times 0.8m$ rectangular domain. Taken from a random function, the pre-generated hydraulic conductivity distribution over the domain has a variance of 1.8, $\ln(K_{max}) = -4.766$, and $\ln(K_{min}) = -12.662$. We triangulate the computational domain into a uniform mesh with 250000 elements and 125751 nodes, which is employed for two sets of computation using the two velocity fields constructed by our new scheme (using both hydraulic head and streamfunction) and by the old scheme (using the hydraulic head only), respectively. To verify the incompressibility condition (mass conservation), we compute the mean horizontal velocity component over the computational domain for the two sets of simulation, obtaining $\bar{u}_{domain(OLD)} = 8.14182 \times 10^{-7}$ and $\bar{u}_{domain(NEW)} = 8.16683 \times 10^{-7}$, respectively. Compared to the mean value at the entrance $\bar{u}_{entrance} = 8.16962 \times 10^{-7}$, the relative error is only 0.0342% associated with our method while this error index reaches 0.3403% corresponding to the old method, about 10 times bigger than using the new approach.

Then, for the transport simulation using the dispersion coefficient at $0.8 \times 10^{-9} m^2/sec$ for both D_x and D_y, $t = 15$ *minutes* as time step, and a source of $c = 1mg/L$ entirely occupying a single triangular element containing the point ($0.05m$, $0.2001m$) and functioning only at the initial instant, we plot in Figure 4 the history of mean mass value over the entire computational domain throughout 300 iterations (equivalent to a period of over 3 days) for the two sets of computation. We remark that, at the end of 300 iterations, the boundary of the rectangular computational domain has not been affected by the transporting solute, physically ensuring the conservation of solute mass within the domain. It is noticed that our new scheme employing both hydraulic head and streamfunction solutions results in a constant mean mass value throughout all 300 iterations while the old scheme relying only on the hydraulic head solution renders the mean mass unceasingly changing during its transport.

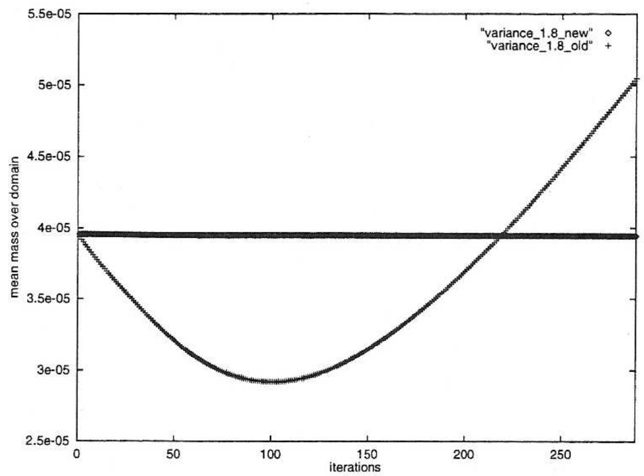

Figure 4: History of solute mass over 300 iterations resulting from two velocity construction methods

Acknowledgments

This work was supported by the Natural Sciences and Engineering Research Council of Canada (NSERC) and by the U.S. National Science Foundation.

References

[1] J. Cao, P.K. Kitanidis, Adaptive-grid simulation of groundwater flow in heterogenous aquifer, *Advances in Water Resources*, **22**, No. 7 (1999), 681-696.

[2] J. Cao, P.K. Kitanidis, An algorithm for solving reactive advection-dispersion problem, *International Journal for Computational Methods in Engineering Science and Mechanics*, **8**, No. 2 (2007), 89-102.

[3] E.O. Frind, G.B. Matanga, The dual formulation of flow for contaminant transport modeling, 1. review of theory and accuracy aspects, *Water Resources research*, **21**, No. 2 (1985), 159-169.